9-2004

Variability and potential sources of predictability of North American runoff

Edwin P. Maurer
Santa Clara University, emaurer@scu.edu

Dennis P. Lettenmaier

Nathan J. Mantua

Recommended Citation
Maurer, E. P., Lettenmaier, D. P., & Mantua, N. J. (2004). Variability and potential sources of predictability of North American runoff. Water Resources Research, 40(9), W09306. https://doi.org/10.1029/2003WR002789

Variability and potential sources of predictability of North American runoff

Edwin P. Maurer
Civil Engineering Department, Santa Clara University, Santa Clara, California, USA

Dennis P. Lettenmaier
Department of Civil and Environmental Engineering, University of Washington, Seattle, Washington, USA

Nathan J. Mantua
Climate Impacts Group, Joint Institute for the Study of the Atmosphere and Ocean, University of Washington, Seattle, Washington, USA

Received 22 October 2003; revised 15 March 2004; accepted 25 June 2004; published 16 September 2004.

[1] Understanding the space-time variability of runoff has important implications for climate because of the linkage of runoff and evapotranspiration and is a practical concern as well for the prediction of drought and floods. In contrast to many studies investigating the space-time variability of precipitation and temperature, there has been relatively little work evaluating climate teleconnections of runoff, in part because of the absence of data sets that lend themselves to commonly used techniques in climate analysis like principal components analysis. We examine the space-time variability of runoff over North America using a 50-year retrospective spatially distributed data set of runoff and other land surface water cycle variables predicted using a calibrated macroscale hydrology model, thus avoiding some shortcomings of past studies based more directly on streamflow observations. We determine contributions to runoff variability of climatic teleconnections, soil moisture, and snow for lead times up to a year. High and low values of these sources of predictability are evaluated separately. We identify patterns of runoff variability that are not revealed by direct analysis of observations, especially in areas of sparse stream gauge coverage. The presence of nonlinear relationships between large-scale climate changes and runoff pattern variability, as positive and negative values of the large-scale climate indices rarely show opposite teleconnections with a runoff pattern. Dry soil moisture anomalies have a stronger influence on runoff variability than wet soil. Snow, and more so soil moisture, in many locations enhance the predictability due to climatic teleconnections. *INDEX TERMS:* 1833 Hydrology: Hydroclimatology; 1860 Hydrology: Runoff and streamflow; 1866 Hydrology: Soil moisture; 1863 Hydrology: Snow and ice (1827); 3322 Meteorology and Atmospheric Dynamics: Land/atmosphere interactions; *KEYWORDS:* runoff, snow, soil moisture, teleconnections, predictability

Citation: Maurer, E. P., D. P. Lettenmaier, and N. J. Mantua (2004), Variability and potential sources of predictability of North American runoff, *Water Resour. Res.*, *40*, W09306, doi:10.1029/2003WR002789.

1. Introduction

[2] To advance the ability to predict floods and droughts, a better understanding is needed of the nature of hydrologic predictability, especially as related to climate. This requires better knowledge of the variability of water cycle components at continental and global scales, which *Hornberger et al.* [2001] identified as a major research need in the coming decade. One common technique used to examine the variability of earth system variables over large regions is principal components analysis (PCA). In hydrological applications, the earliest uses of PCA were for reducing a set of correlated predictors in regression analysis to a minimum number of uncorrelated variables that are linear combinations of the original variables [e.g., *Rice*, 1967; *Snyder*, 1962; *Wallis*, 1965; *Wong*, 1963]. The earliest applications of PCA were to atmospheric fields, and it follows that interpretation of principal component (PC) loadings, representing uncorrelated modes of variability, also were first developed for these variables [e.g., *Grimmer*, 1963]. For variables directly related to land surface hydrology, spatial PC loading plots were first evaluated for meteorological variables such as precipitation [*Kutzbach*, 1967], while the application of spatial analysis using PCA to other land surface variables appeared later.

[3] The usefulness of PCA for both reducing the dimensionality of large data sets and providing a graphical display of spatially coherent modes of variability has motivated the use of PCA in more recent analyses of streamflow [*Piechota et al.*, 1997; *Lins*, 1997; *Guetter and Georgakakos*, 1993; *Bartlein*, 1982], soil moisture [*Wittrock and Ripley*, 1999],

0043-1397/04/2003WR002789

snow water equivalent [*Derksen et al.*, 1997; *Cayan*, 1996], drought indices [*Cook et al.*, 1999], and for all components of the land surface water budget [*Famiglietti et al.*, 1995].

[4] *Lins* [1997] (hereinafter referred to as L97) identified 11 dominant regions of streamflow variability, using PCs of monthly streamflow derived from gauge records. Regionally coherent patterns were examined to identify their evolution and decay, giving an indication of the potential predictability of these patterns at monthly lead times based on their persistence from month to month.

[5] With respect to streamflow, one of the main difficulties in the use of PCA is that as opposed to point measurements of soil moisture, snow, or precipitation, for example, streamflow represents an integrated quantity from a contributing basin. Thus streamflow variability detected at a stream gauge does not identify the source of that variability. Furthermore, as discussed by L97, the inherent asymmetry in the location of the stream gauges that collect the data, and the widely varying areas they represent, lead to some uncertainty in the interpretation of the resulting plots of PC loadings. *Guetter and Georgakakos* [1993] note that another shortcoming of using streamflow observations in PCA is that, for many rivers, streamflow observations reflect the effects of regulation and diversions that distort the natural patterns of variation. While L97 used a data set of unimpaired observed streamflows, where the effects of regulation and diversion are minimal, the L97 data set does exhibit the other complications noted above.

[6] It has been well known for many decades that soil moisture and snow play key roles in predicting the hydrologic response of the land surface [e.g., *Linsley and Ackerman*, 1942; *Church*, 1937]. Advances in understanding the teleconnections of sea surface temperature (SST) and persistent or predictable climate anomalies to the land surface have provided opportunities for improving predictability of runoff in some regions [e.g., *Hamlet and Lettenmaier*, 1999; *Garen*, 1998]. Thus understanding teleconnections of remote SST and climate conditions to runoff variability and the contribution of soil moisture and snow to this variability will allow an assessment of the opportunities for improving runoff predictability in different regions (for example, where better definition of antecedent soil moisture conditions can provide a substantial benefit to runoff prediction, and where and when it may be less important).

[7] In this study, we address three questions: (1) Do different patterns of runoff variability emerge with spatially distributed runoff data as compared to the irregularly spaced gauge data of L97? (2) What are the SST and climatic teleconnections to the patterns of runoff variability? (3) Where and at what lead times are the soil moisture and snow conditions significantly related to the runoff variability?

[8] To address the first question, we analyze a spatially distributed runoff data set derived from a macroscale hydrology model for the continental United States. The model is calibrated using observed streamflow from large river basins in the continental United States [*Maurer et al.*, 2002]. By using the gridded runoff data from the data set (described in detail by *Maurer et al.* [2002] and summarized in section 2) each grid cell represents a comparable area, so the asymmetry of streamflow observations will not affect the PCA results. Further, because runoff from the derived data set, when routed through the channel network to specified stream gauges reproduces observed streamflows (adjusted for management effects where necessary) reasonably well, the derived modes of variability arguably are representative of the natural variability in the hydrologic system.

[9] To address the second question, we derive statistical relationships between each of our identified seasonal runoff variability patterns and large-scale climate indices that capture the anomalous states of sea surface temperature (SST) and surface atmospheric pressure. The persistence of these signals and their teleconnections to land surface hydrologic response can provide valuable runoff predictability. To address the third question, we determine the statistical significance of connections between land surface variations (soil moisture, SM and snow water equivalent, SWE) at each grid cell in the domain and variations in each defined runoff pattern.

[10] Potential predictability of runoff could be explored by evaluating the sources of predictability of the main driving mechanism for runoff, precipitation, which might then be related to the runoff variability. While this would reveal locations where precipitation and runoff are out of phase, it would be of less value as a predictive tool, since for example, many of the climate indices affect both precipitation and temperature, both of which affect runoff. Our aim is in this study is to evaluate observable states that are, to varying extents, available to forecasters (SST anomalies, atmospheric conditions, land surface water storage) at different lead times, and to evaluate their predictive capability for regional runoff. For this study, we have chosen to compare directly the variability of runoff to a suite of SST, atmosphere, and land surface state variables, which reflects the ability to use these predictors directly for runoff forecasting.

2. Data and Methods

2.1. Runoff, Snow, and Soil Moisture Data

[11] The runoff, snow, and soil moisture data used in this study are the derived products archived by *Maurer et al.* [2002], which cover the period 1950–2000 for that portion of North America between latitudes 25°N and 53°N at 1/8 degree spatial resolution. The data were derived using the Variable Infiltration Capacity (VIC) land surface hydrology model [*Liang et al.*, 1994] driven by observed and observationally based meteorological forcing data at a three hour time step. The observed precipitation and temperature are station observations throughout the domain (see *Maurer et al.* [2002] for the details on derivation of other forcing variables and model parameterization). The derived runoff was routed through defined stream networks and was shown to produce streamflows that compared favorably with observations at the outlets of river basins across the continental United States. The SWE and SM data used in this study were also produced by the model, and were shown by *Maurer et al.* [2002] to be plausible values when compared with available observations. *Maurer et al.* [2002] present comprehensive comparisons of the simulated data (runoff, soil moisture, and snow); for basins varying in size from 7000 km^2 to over 1,400,000 km^2. They show that simulated runoff has an average absolute bias of 3.1%, and

an RMSE of 34.5% (based on monthly simulated and observed streamflow values for a 10-year period), when compared with observations. The average monthly hydrographs are shown to correspond well to observations in basins throughout the domain. With forcing meteorology based on observations, reasonable reproduction of observed streamflow and the physically based model VIC structure we assert that derived variables are also realistically simulated, an assertion that is borne out by favorable comparisons of model output to observed soil moisture fluxes in Illinois and satellite observed snow extent (see *Maurer et al.* [2002] for details on the data derivation and output comparisons).

[12] For this study we aggregated the original 3-hourly runoff values to seasonal averages (seasons are defined by 3-month sequences as winter, December–February (DJF); spring, March–May (MAM); summer, June–August (JJA); and fall, September–November (SON)) and aggregated spatially from the 1/8 degree native spatial resolution of the data set to $^1/_2$ degree spatial resolution (resulting in 5051 individual grid cells), in order to reduce array sizes and produce a more computationally tractable data set.

2.2. Climate Indices

[13] At seasonal to interannual scales, the El Niño–Southern Oscillation (ENSO) is the best known and most prominent predictable climate signal [*Rasmussen and Wallace*, 1983]. Many studies have documented teleconnections of ENSO [*Trenberth*, 1997] to land surface variables affecting hydrologic variability including temperature [*Higgins et al.*, 2000], precipitation [*Kahya and Dracup*, 1993; *McCabe and Dettinger*, 1999], and streamflow [*Cayan et al.*, 1999]. These documented teleconnections have been used to investigate potential improvements in predictability of runoff by incorporating knowledge of ENSO phase [*Wood et al.*, 2002; *Baldwin*, 2001; *Garen*, 1998]. To characterize the state of the ENSO in this study, the Niño 3.4 index was obtained from: ftp://ftp.ncep.noaa.gov:/pub/cpc/wd52dg/data/indices/. The Niño 3.4 index characterizes the tropical Pacific SST anomalies between latitudes 5S and 5N and longitudes 170W and 120W, a region defined to capture ENSO-related SST anomalies [*Barnston et al.*, 1997].

[14] The Pacific Decadal Oscillation (PDO) [*Mantua et al.*, 1997] has received considerable attention in recent years, and has been shown to be a predictor for Columbia River streamflow [*Hamlet and Lettenmaier*, 2002] in the Pacific Northwest. Incorporation of PDO state in water supply forecasts has been shown to produce significant value for water management [*Hamlet et al.*, 2002]. The PDO index, which is defined as the leading PC of monthly SST anomalies in the North Pacific Ocean north of latitude 20N, was obtained from ftp://ftp.atmos.washington.edu/mantua/pnw_impacts/INDICES/PDO.latest.

[15] Recent studies show that additional predictability of air temperature and precipitation, particularly in winter, can be obtained over portions of the United States by accounting for the modes of the Arctic Oscillation (AO) [*Thompson and Wallace*, 1998], which some have argued is more or less equivalent to the North Atlantic Oscillation (NAO) [e.g., *Higgins et al.*, 2000; *Rohli et al.*, 1999]. To characterize the state of the AO, an AO index was obtained (from http://www.atmos.colostate.edu/ao/Data/ao_index.html; see *Thompson and Wallace* [1998, 2000] for details). This AO index is the leading PC of the sea level pressure anomalies north of latitude 20N. *Higgins et al.* [2000] show that incorporation of the AO into climate prediction schemes shows promise, especially in winter.

[16] The NAO, encompassed by the AO, is the normalized pressure difference between two stations, one in the Azores and one in Iceland [*Hurrell*, 1995].The NAO index used in this study was obtained from http://www.cgd.ucar.edu/~jhurrell/. The NAO has been shown to be related to changes in Northern Hemisphere temperatures and precipitation, including North America [*Hurrell et al.*, 2003; *Lin and Derome*, 1998], especially on the East Coast [*Wettstein and Mearns* 2002]. *Higgins et al.* [2000] present the argument that the AO encompasses the NAO, and hence are closely related. Although the NAO and AO are closely related, there is evidence that some regional teleconnection signatures of the AO and NAO are distinct [e.g., *Rogers et al.*, 2001], and therefore both are retained in this study.

[17] The North Pacific (NP) index [*Trenberth and Hurrell*, 1994] is the area-weighted sea level pressure over the region 30°–65°N, 160°–140°E. This is an indicator of the intensity of the Aleutian low pressure, which was indicated by L97 to be connected to regional streamflow variability in the western United States. Historical values for this index were obtained from http://www.cgd.ucar.edu/~jhurrell/np.html. The NP can also be considered a sea level pressure-based index depicting the Pacific-North American Index (PNA) pattern, which is based on 500 hPa atmospheric pressure patterns [*National Research Council*, 1998], and is essentially a mirror image of the PNA [*Hare and Mantua*, 2000].

[18] The Atlantic multidecadal oscillation (AMO) has recently been found to be correlated with predictable patterns of rainfall across the United States [*Enfield et al.*, 2001]. The AMO is derived from the sea surface temperature anomalies in the Atlantic Ocean north of the equator. Historical values for the AMO index were obtained from http://www.cdc.noaa.gov/ClimateIndices/.

2.3. Principal Component Method

[19] On the basis of the success of past studies in identifying physically meaningful spatial patterns of variables including runoff using PCA (see references cited in section 1), we chose PCA to characterize the runoff variability for this analysis. By defining the runoff patterns with PCA prior to the other analyses we are able to define coherent, regional patterns for each season, against which all climate signals and land surface states can be compared. PCA was performed on the gridded seasonal runoff data, arranged into a matrix with one column for each grid cell in the domain and one row for each year (four separate matrices were prepared: one for each season). The correlation matrix was specified in the PCA to avoid loadings being focused exclusively in regions with high runoff. Following the derivation of the loading matrices, we applied an orthogonal varimax rotation following *Richman* [1986], similar to the approach used by L97. This PC rotation concentrates the loadings for each PC onto the most influential variables, while retaining the orthogonality of the PCs. The number of PCs to rotate (10) was selected using a Monte Carlo approach applying the Rule N technique [*Preisendorfer and Barnett*, 1977; *Overland and Preisendorfer*, 1982]. The runoff data matrix was then

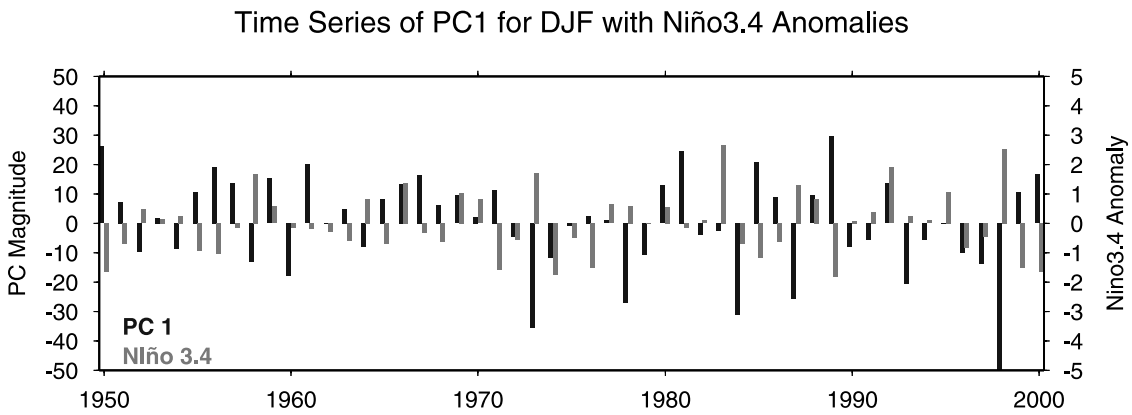

Figure 1. Time series of PC1 for December–February (DJF) and the Nino 3.4 index for the period of 1950–2000.

projected onto the rotated PC loadings matrix to obtain a time series for each rotated PC and each season.

2.4. Lead Times

[20] The relationship of each PC to each climate signal (or soil moisture state) is established at different lead times. Lead times are defined as by *Maurer and Lettenmaier* [2003], where the lead time indicates the number of intervening seasons between the date on which the climate signal (or soil moisture or snow state) is established and the first day of the season for which the PC time series is being evaluated. Soil moisture, snow state, and climate indices are all set to their values on the first day of the season at the specified lead time. In other words, for a lead of zero and PC of DJF runoff, the climate signals used are those occurring on the first day of the season, 1 December. In this sense, the utility of the climate signals as predictors of runoff variability, at lead times up to four seasons, is assessed.

2.5. Climate Signal Teleconnections to Spatial Runoff Patterns

[21] The significance of the teleconnections of each climate signal to runoff is established for each (rotated) PC for each climate signal at each lead time. Since the climate signals can exhibit strong terrestrial teleconnections in one phase, and weak teleconnections in an opposing phase, a direct linear correlation could fail to detect important signals. For example, a time series of the first PC with the Niño 3.4 index is shown in Figure 1, which shows an apparent tendency of low Niño 3.4 values to coincide with high PC magnitudes, although the relationship for high Niño 3.4 values is less clear. For this reason, we evaluate the data as shown in Figure 2, which plots the 10 highest and 10 lowest values of a potential predictor of runoff, in this instance the Niño 3.4 index, against the corresponding values of the time series of one of the runoff PCs. Figure 2 is for illustration only and shows that the PC magnitudes are different from zero in one case and not in the other (as opposed to whether the pattern itself is weak or strong in this particular case). In this example, the stronger apparent correspondence between PC magnitude and low Niño 3.4 values is shown (with 9 of 10 points exceeding zero), while the relationship is weaker for high values (scattered around the horizontal zero line). These two sets of 10 points are each evaluated separately to determine if they are significantly different from zero, using a t test at a 95% confidence level. In this manner both phases are independently assessed for their teleconnection to each mode of runoff variability. The technique described above to determine the existence of a relationship between positive and/or negative phases of any climate signal and any of the runoff patterns is a composite analysis, where the mean of the PC magnitudes corresponding to the 10 highest and 10 lowest climate signal magnitudes are tested independently. Therefore negative and positive phases of Niño 3.4 (or any climate index) may affect different spatial regions, and it can be found significant in one phase regardless of its significance in the opposite phase.

2.6. Snow and Soil Moisture Contribution to Runoff Variability

[22] Since the SWE and SM data used in this study are complete time series at each grid cell, each grid cell can be

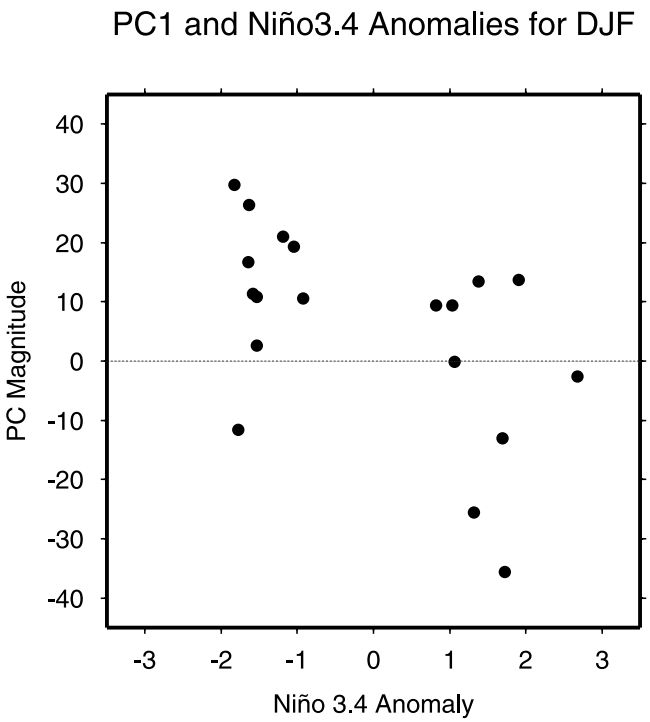

Figure 2. Scatterplot of the 10 highest and 10 lowest Nino 3.4 values in the period 1950–2000 against the ordinate values of the magnitude of PC1.

evaluated individually for its contribution to the mode of runoff variability represented by each PC loading pattern. This is performed for each grid cell in a manner identical to that used for the climate indices, where the PC magnitudes associated with the 10 highest and 10 lowest SWE or SM values at each grid cell are evaluated with a t test to determine if they are significantly different from zero at a 95% confidence level.

3. Results and Discussion

[23] The results are presented below in a sequence following their introduction above, namely, (1) the runoff variability patterns, (2) the climate teleconnections to each one, and (3) locally significant SWE and SM connections to each pattern. In the text that follows, variability of runoff is described as coherent patterns of runoff variability. Where a particular phase of a climate signal shows a statistically significant relationship to a pattern of runoff, it is referred to as a teleconnection.

3.1. Patterns of Variability

[24] The domain used in this study differs from that of L97, extending beyond the conterminous United States, and this study uses gridded runoff as opposed to streamflow observations. The 11 regional patterns identified in this study are shown in Figure 3. These patterns do not all appear in each season, and vary somewhat from season to season. Individual maps in Figure 3 for each region are only shown for the seasons in which a coherent runoff pattern exists in the region. The lack of a continental-scale runoff pattern in a particular region and season indicates a lack of large-scale coherent variability, and implies less influence from large-scale forcing and more runoff variability due to local, spatially heterogeneous factors, such as soil textures and local weather patterns.

[25] Figure 3 reveals some different patterns of runoff variability and extends some of the patterns identified by L97 into Canada and Mexico. Because of the differing time periods of the studies (1941–1988 for L97; 1950–2000 for this study) there are difficulties in comparing the two studies. However, the comparisons do hint at important differences, which might be the basis for future studies with expanded data sets.

[26] Note that as these regional runoff patterns vary in space from season to season, they are not necessarily the same PC in each season. In other words, the PC time series between two consecutive seasons in any region may not be strongly correlated, reflecting differing sources of variability. For example, for the Mid-Atlantic region, the Pearson correlation coefficient of 0.5 between winter and spring PCs is highly significant, while between spring and summer the two are uncorrelated. Where a pattern is referred to as shifting spatially from season to season, this refers not to a translating PC, but rather to a similar pattern of coherent variability existing in the same general region in a subsequent season.

[27] One example of differences between L97 and this study is the East/Mid-Atlantic/Gulf pattern, identified in this study and also by L97, shown in Figure 3a. L97 identify two separate patterns: one for the Mid-Atlantic that is prominent in the winter and fades by late spring and one for the Gulf that is strongest in summer and autumn. In this analysis these are less distinguishable, appearing as one form that migrates south in the spring and summer. Our study identifies an additional runoff pattern that appears, in part, because our study domain extends into Canada. There is a northward shift in the center of the New England/Quebec runoff pattern (Figure 3e) during fall and winter that is absent in L97's results. Since L97 bases streamflow patterns of streamflow observations from 1941–1988, the record lengths in L97 and this study are comparable, indicating the differences are most likely attributable to the use of gridded runoff rather than gauge station observations. While the differing periods of study may affect this inference, with record lengths of 48–50 years there should be stability in the patterns, and we note that 39 years of record are common to the two studies.

[28] Our results suggest that the ability to identify patterns of runoff variability using observations alone may be limited in areas with sparse stream gauge networks. For example, in the northern Great Plains the distributed runoff values used in this study reveal variability not detectable with the sparse gauge observations. Where L97 identified an Upper Mississippi river pattern that persisted throughout the year, in this study it is prominent only in winter (Figure 3g). Two additional patterns appear to the north and west, however: the Upper Missouri/Canada (Figure 3h) and Lower Missouri (Figure 3k) patterns. The importance of characterizing runoff variability in these regions is highlighted by the devastating impacts of recent events in this area such as the 1993 Mississippi River flood [*Parrett et al.*, 1993] and the April 1997 Red River flood [*Bell and Halpert*, 1998].

3.2. Potential Sources of Runoff Predictability

[29] The statistically significant climate teleconnections for each of the 11 identified runoff patterns are summarized in Table 1 for each season and each lead time and for each phase of the climate signal. Note that Table 1 does not show statistically significant correlations but, rather, PC magnitudes that are significantly different from zero at the given significance level, as described in section 2.5. Table 1 clearly shows the general deterioration of climate signal teleconnections to runoff with increasing lead time, with most runoff patterns having fewer significant climate teleconnections at higher lead times.

[30] One exception to this is climate teleconnections to the northern patterns of runoff variability in DJF (New England/Quebec and Upper Missouri/Canadian Prairie), where the first significant climate teleconnection to DJF runoff is at leads of two to three seasons. This can be explained by the fact that the relatively small amount of runoff produced during DJF in far northern regions is mostly soil moisture-derived base flow (since most DJF precipitation falls as snow, appearing as runoff in the spring and summer), with the soil moisture resulting from meteorological forcing in prior seasons. A similar effect was also identified by *Lettenmaier et al.* [1994] where up trends in precipitation, occurring mostly in the autumn, accounted for up trends in winter streamflow, especially across the northern and midwestern United States. Trends existing in both the runoff PC time series and the soil moisture would tend to increase the correlation as well.

[31] Table 1 also shows the presence of many significant climate teleconnections to DJF and MAM runoff for more

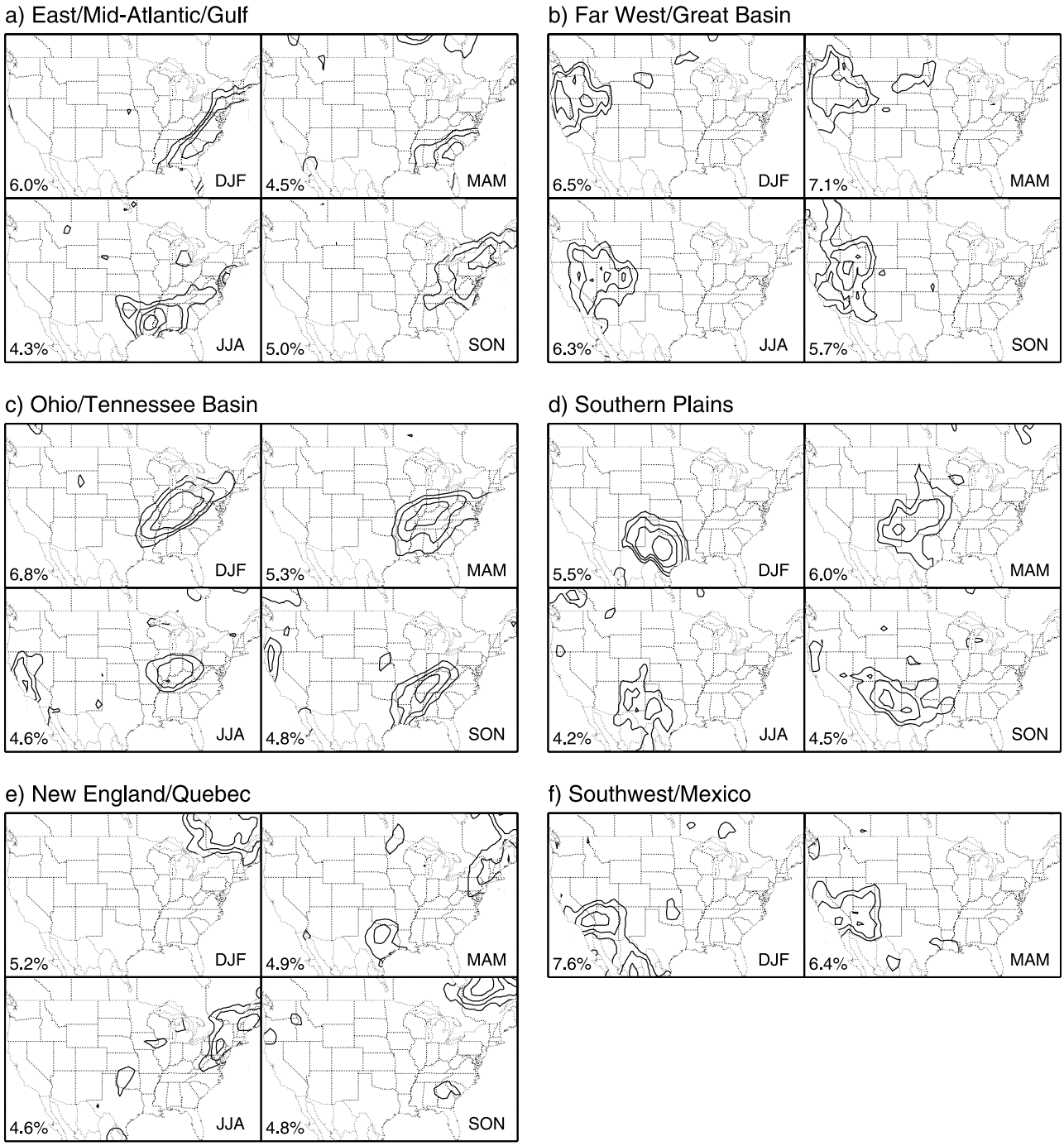

Figure 3. Spatial plot of the runoff PC loadings, grouped into regions as defined. The number in the lower left corner of each panel is the percent of total runoff variance explained by the exhibited pattern.

southern regions, and to MAM and JJA runoff for northern and high elevation (more snow-dominated) regions, where the lag between climatic anomalies and runoff anomalies tends to be greater. Another general feature shown in Table 1 is the general decline in Niño 3.4 as a significant influence on runoff variability at lead times of two seasons or longer. This is consistent with the observation of *Barnston et al.* [1999], who note that ENSO events typically develop in spring to early summer and have their greatest influence in winter. This suggests that a lead of two seasons, corresponding to a 7.5 month lead time (2 intervening seasons plus 1.5 months to the midpoint of the "forecasted" season) would be at the outer limit of predictability of runoff using ENSO, at least from a persistence analysis as used in this study. The exception to this is for the Pacific Northwest pattern, where the long delay between winter snowfall and summer snowmelt effectively extends the forecast horizon by several months.

[32] The AO and NAO are shown in Table 1 to be significantly related to patterns of runoff variability at long lead times and for patterns across the domain. This seems to confirm the assertion by *Higgins et al.* [2000] that forecasts

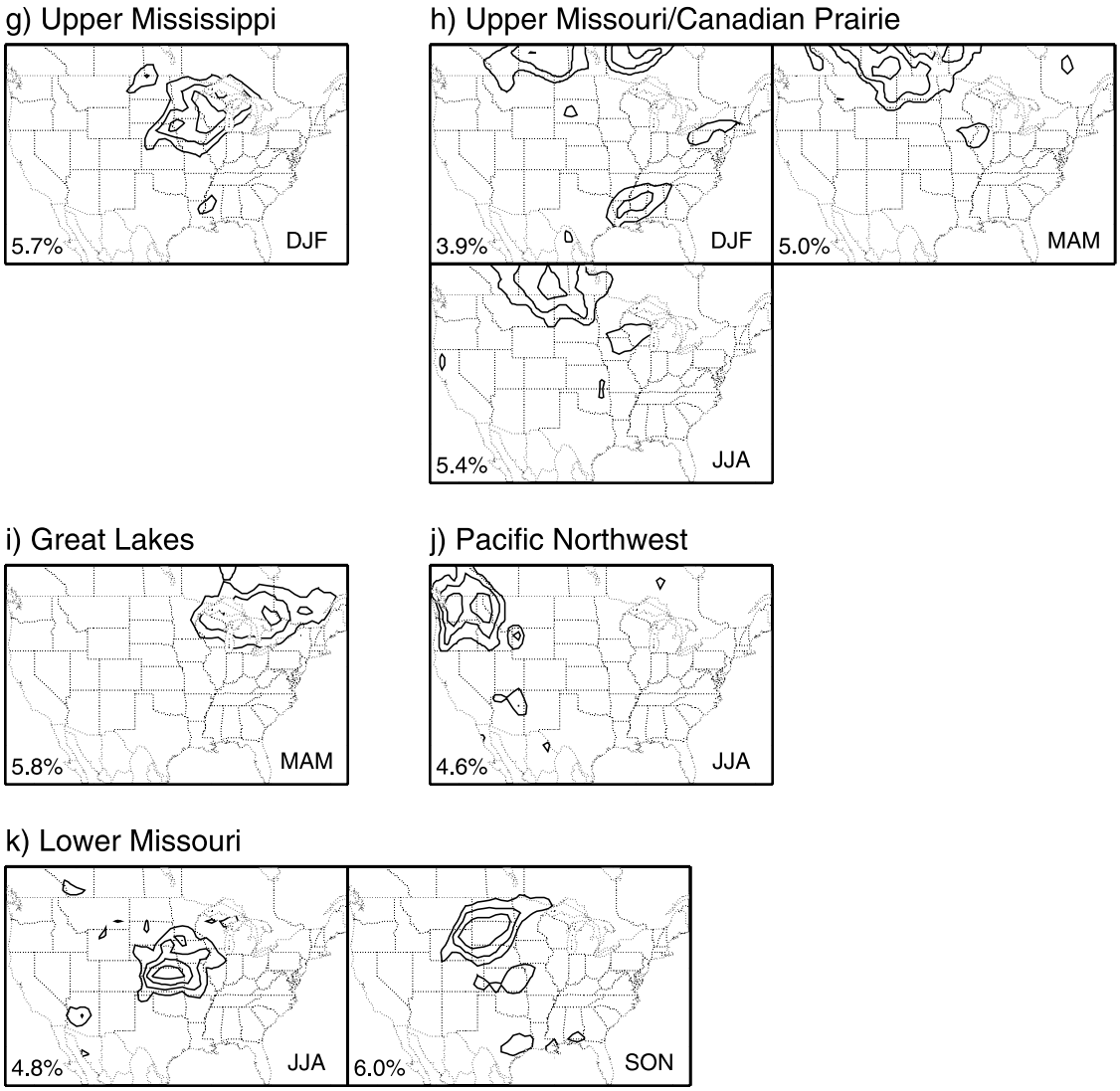

Figure 3. (continued)

of the AO could result in increased climate predictive skill, in particular for runoff.

[33] In most cases one phase of a climate signal has a significant teleconnection to runoff variability while its opposite does not. For example, Table 1 shows the PDO in its negative phase being related to runoff variability in the Pacific Northwest through two seasons, but no significant relationship to PDO in its positive phase. Although *Hamlet and Lettenmaier* [1999] note influence of PDO in both its positive and negative phase on Columbia River streamflow (the major component of the Pacific Northwest runoff pattern), this is complicated by the nonlinear reinforcing of effects of the PDO and ENSO, where their effects when in phase are substantially more pronounced than when out of phase.

[34] One example of nonlinear climate teleconnections to the regional runoff patterns is seen for the East/Mid-Atlantic/Gulf runoff pattern: the negative Niño 3.4 phase is related to DJF runoff, while the positive phase is related to MAM runoff. The positive Niño 3.4 phase, corresponding to El Niño conditions, has been found to correspond to wetter and stormier winter conditions on the East Coast [e.g., *DeGaetano et al.*, 2002]. Table 1 shows for the East/Mid-Atlantic/Gulf pattern the positive Niño 3.4 phase is correlated with MAM runoff at leads of zero and two seasons. In other words, the positive Niño 3.4 phase on 1 March and the previous 1 September are found to be statistically related to MAM runoff. This illustrates how teleconnections of SST anomalies to precipitation or temperature variability can be translated at the land surface into runoff variability at a later time.

3.3. Land Surface Connection to Runoff Variability

[35] The SWE and SM influences on the patterns of runoff variability were determined for each season and lead time. Of particular interest are areas where SWE and/or SM show a significant relationship to a runoff pattern that does not benefit from significant climate teleconnections. Because the array of climate indices used in this study is not exhaustive, where we found no significant relationship of a runoff pattern to climate indices below, this result is specific to the indices we considered.

3.3.1. SWE Influence on Runoff Pattern Variability

[36] The influence of SWE on runoff variability must follow the patterns of snowmelt. Since snowmelt generally occurs in MAM and JJA, these are the only seasons for

Table 1. Summary of Climate Signals Exhibiting 95% Significant Teleconnection to the Indicated Pattern of Runoff Variability for the Designated Season and Lead Time[a]

	Lead 0	Lead 1	Lead 2	Lead 3	Lead 4
			East/Mid-Atlantic/Gulf		
DJF	Nino3.4(−)	Nino3.4(−), PDO(−)	AMO(+)	AO(−), NAO(−)	
MAM	Nino3.4(+)		Nino3.4(+)		
JJA	PDO(+)			PDO(−)	
SON			AO(−)		AO(−)
			Far West/Great Basin		
DJF		NP(+)			
MAM					AO(−)
JJA	AO(+)	NAO(−), NP(+), PDO(−)			Nino3.4(−), AMO(+)
SON		AO(+)	NP(−)		
			Ohio/Tennessee Basin		
DJF	NP(−)			AO(−), AMO(+)	
MAM	PDO(−)	Nino3.4(−)			
JJA	PDO(±)	NP(+), PDO(−)			
SON	AMO(+)	AMO(+)	AO(+), AMO(+)		
			Southern Plains		
DJF	PDO(−)	Nino3.4(−), PDO(−), AMO(−)			NAO(+)
MAM	Nino3.4(+), PDO(−)	Nino3.4(+), PDO(+)		Nino3.4(+)	
JJA	PDO(−)	AO(+)			AO(−)
SON	Nino3.4(−)				
			New England/Quebec		
DJF				NP(−)	
MAM	NAO(+)			AO(−), NAO(−)	NAO(−)
JJA	NAO(−)		PDO(−)	PDO(−)	NAO(−)
SON	PDO(+)	AO(+), Nino3.4(+)	AO(+), PDO(−)	AMO(+)	
			Southwest/Mexico		
DJF	NP(−)	Nino3.4(−)	PDO(−), AMO(+)	PDO(−)	PDO(−), AMO(+)
MAM	Nino3.4(±), PDO(−)	AO(+), NAO(−), Nino3.4(±)	Nino3.4(−)	Nino3.4(−), AMO(+)	AMO(+)
			Upper Mississippi		
DJF	PDO(−)			NP(−)	PDO(+)
			Upper Missouri/Canadian Prairie		
DJF			NAO(−)		
MAM	PDO(+)		PDO(+)	PDO(+)	AO(+)
JJA					
			Great Lakes		
MAM	AO(−), AMO(−)	NAO(+)			AMO(+)
			Pacific Northwest		
JJA	PDO(−), AMO(−)	PDO(−)	Nino3.4(−), PDO(−), AMO(±)	Nino3.4(±)	
			Lower Missouri		
JJA	AO(+)	AMO(−)			AMO(−)
SON					AO(+)
			Upper Mississippi		
DJF		AMO(−)			

[a]See text for definition of the climate signals. A (+) indicates the positive phase of this index is significantly related to the runoff pattern (see section 2.5 for a description of the significance test), a (−) indicates the negative phase, and (±) indicates both phases. Rows indicate runoff season, and columns indicate lead time in seasons. DJF, December–February; MAM, March–May; JJA, June–August; SON, September–November; AMO, Atlantic Multidecadal Oscillation; AO, Arctic Oscillation; PDO, Pacific Decadal Oscillation; NAO, North Atlantic Oscillation; NP, North Pacific index.

which many grid cells exhibit significant correlation with any patterns of runoff variability. Figure 4 shows the patterns of variability influenced by SWE for MAM at a lead of zero seasons and the grid cells where SWE is significantly related to the runoff variability. For the Far West pattern, Table 1 indicates that no significant climate teleconnections were found among the suite of climate indices included in this study, so the predictability of runoff added by SWE is potentially of greater importance. For the Great Lakes pattern, the AO negative phase also provides predictability, but since SWE influences runoff in both high and low conditions, SWE adds a measure of predictability for this runoff pattern in addition to that achieved by the climate teleconnections. Figure 5 shows the connection between SWE and JJA runoff in the Pacific Northwest, where JJA runoff is essentially fully determined by the late spring snowpack.

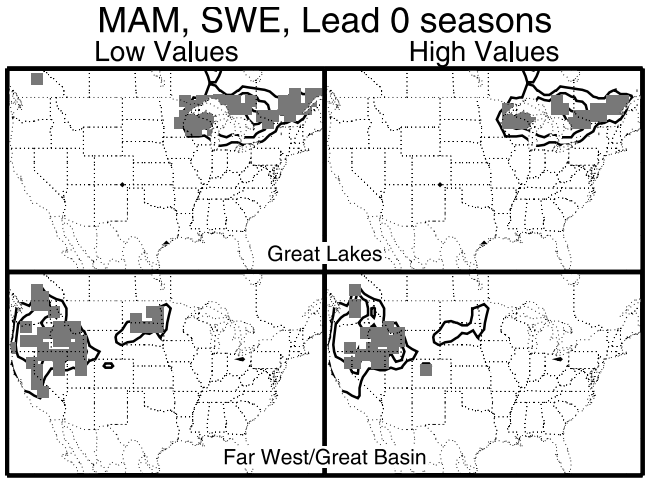

Figure 4. For the indicated runoff patterns (identical to those in Figure 3 for the specified season), shaded blocks indicate grid cells with statistically significant relationships of SWE with runoff pattern variability for the season March–May (MAM) and lead time of zero seasons. This relates the MAM runoff variability, expressed in the PC time series, with the SWE anomalies at the prior time indicated by the lead time.

[37] Figure 6 is the same as Figure 5 but for a lead of one season (i.e., SWE determined on 1 March). It is evident that SWE still explains much of the runoff variability for these patterns, but more so for conditions of low SWE than high SWE. One explanation for this is that high SWE years replenish soil moisture with a portion of the snowmelt, thus reducing the influence of SWE on the JJA runoff for the current year. Low SWE anomalies will always affect the following season's runoff. Although not shown, this SWE connection to runoff variability in this region persists through two seasons.

3.3.2. SM Influence on Runoff Pattern Variability

[38] As observed by *Maurer and Lettenmaier* [2003], runoff predictability due to soil moisture, at least in the Mississippi River basin, tends to be highest in areas and during periods with low runoff, at least partially because any runoff tends to be derived from soil moisture drainage. This is seen in Figure 7, which shows the runoff patterns displaying SM connections at a lead of zero seasons. For the Ohio/Tennessee Basin pattern, low SM is significantly related to the variability of the runoff pattern, while high SM is not. This indicates that dry soils on 1 December have a greater impact on DJF runoff than wet soils in this region.

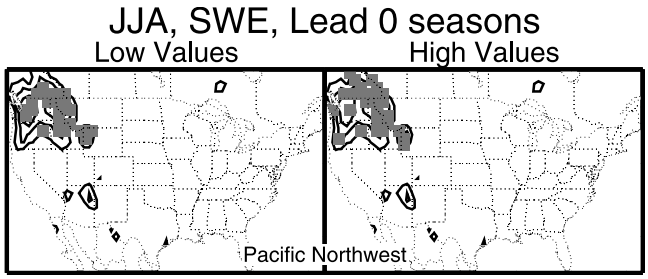

Figure 5. Same as Figure 4, but for season June–August (JJA).

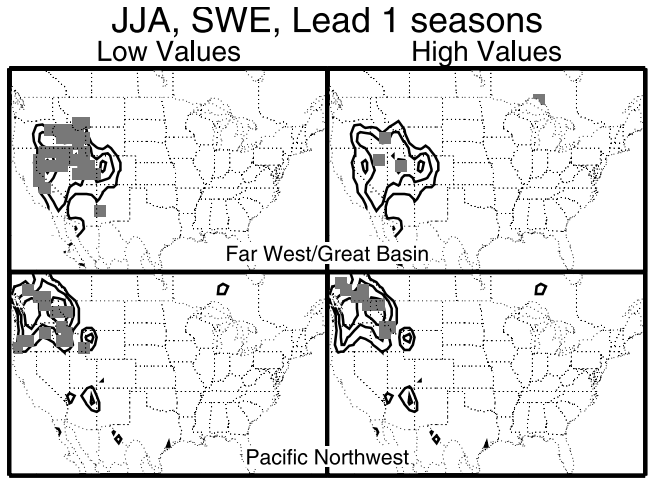

Figure 6. Same as Figure 4, but for season JJA and a lead time of one season.

Table 1 shows the NP(−) index related to this pattern. A negative NP index corresponds to a positive PNA index, which is strongly correlated to (dry) below average precipitation anomalies in this region [e.g., *Leathers et al.*, 1991]. This means that the SM information overlaps with the knowledge already gained by the NP index. For the New England/Quebec and Upper Missouri/Canadian Prairie patterns, strong SM connection to runoff is apparent, while no significant climate signal is shown in Table 1, indicating SM state is potentially a more valuable predictor of DJF runoff in these regions. As with the Ohio/Tennessee pattern, the Southwest/Mexico pattern also shows many grid cells with significant relationships to runoff variability with low SM, but substantially fewer for high SM.

[39] MAM SM connections are shown in Figure 8, also for a lead of zero seasons. For all patterns both high and low SM values maintain connections to runoff variability, so for those cases where one phase of a climate signal also has a significant teleconnection to runoff variability, SM can be a valuable predictor, adding unique information, since any particular phase of a climate signal will be correlated with one SM extreme state at most. Figure 9 corresponds to JJA runoff variability. SM is significantly related to these runoff patterns for both high and low SM values, and again where only one phase of any climate signal is indicated in Table 1 as explaining runoff pattern variability, the SM augments this information for improved predictability. Although not illustrated, our results indicated that SM again explains significant SON runoff variability for both high and low values for a lead of zero seasons for the New England/Quebec and Far West/Great Basin patterns.

[40] SM influence on runoff variability begins to decline at a lead of one season. For MAM runoff, Figure 10 can be compared to Figure 8 to illustrate the decline in the number of grid cells showing a significant relationship to the pattern of runoff variability. In Figure 10, SM may be the primary source of predictability for MAM runoff variability for the Far West/Great Basin pattern since there is no climate teleconnection indicated in Table 1 nor is there a SWE relationship for MAM at a lead of one season.

[41] The SM connection to JJA runoff variability at a lead of one season is shown in Figure 11. Here the one season

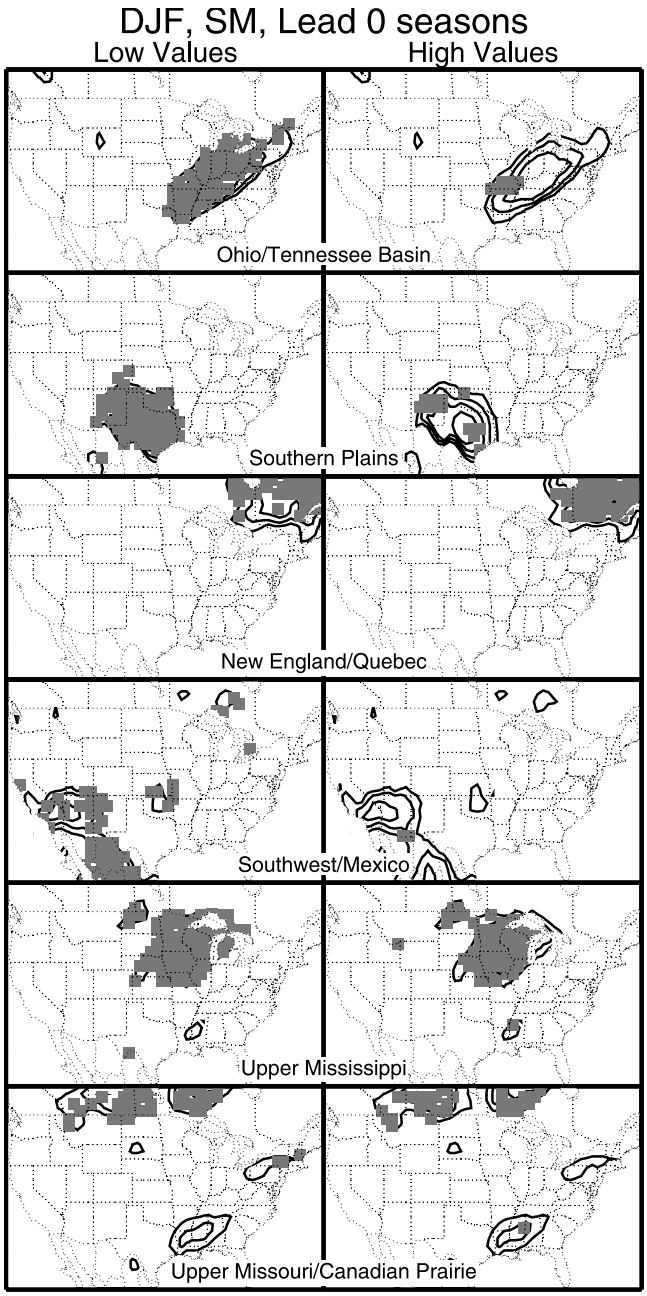

Figure 7. For indicated runoff patterns, shaded blocks indicate grid cells with statistically significant relationship of SM with runoff pattern variability for the season DJF and lead time of zero seasons.

lead time correlations are considerably weaker than those at a lead of zero seasons (Figure 9). Also, since both of the runoff patterns shown in Figure 11 also share SWE and climate signal contributions to explaining runoff variability, the SM plays a smaller role in predictability of JJA runoff at a lead of one season. Figure 12 shows that for the Far West/Great Basin runoff pattern, SM is significantly related to the SON runoff variability, though this is a season of declining runoff, so the predictive capability affects a small quantity of runoff and therefore will have lessened value. Although not shown, the level of SM connection to the runoff variability in Figure 12 continues at approximately the same

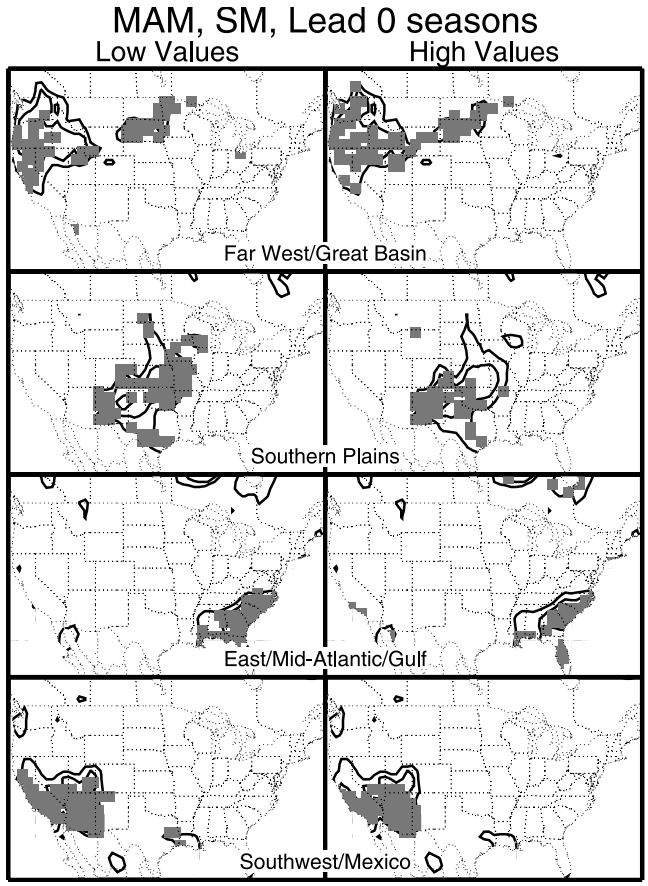

Figure 8. Same as Figure 7, but for season MAM.

level through a lead of two seasons, showing that the SM levels the previous 1 March can be a significant predictor of the following SON runoff variability in portions of this region.

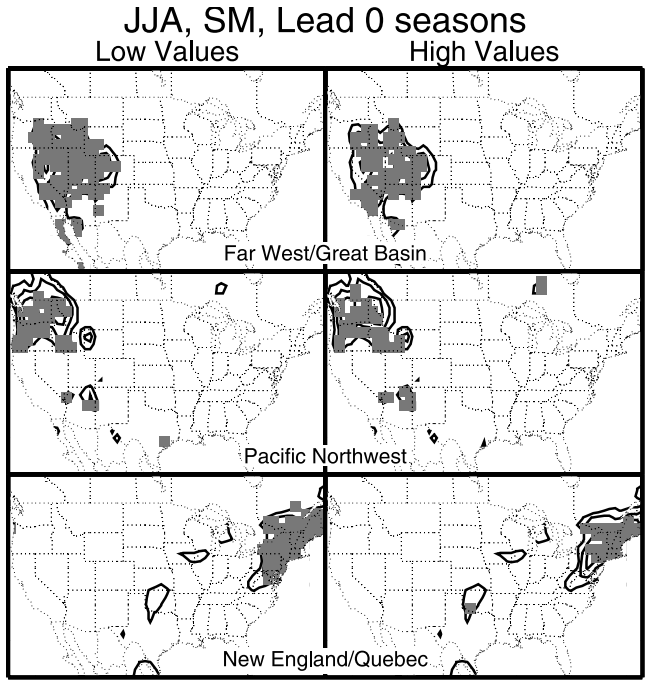

Figure 9. Same as Figure 7 but for season JJA.

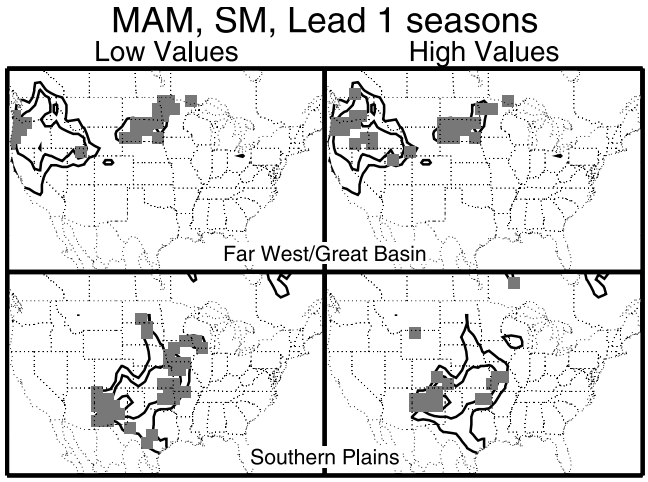

Figure 10. Same as Figure 7, but for seaosn MAM and a lead time of one season.

[42] Figure 13 shows the SM influence on three DJF runoff patterns at a lead of two seasons. Both the Ohio/Tennessee and the Upper Mississippi patterns have no significant climate teleconnections for DJF at this lead time (see Table 1), so SM has the potential to provide valuable information on runoff variability not available from other sources, at least for the limited regions within each pattern showing significant SM connection.

4. Conclusions

[43] We examined the space-time variability of runoff over North America between latitudes 25 N and 53 N. Comparison of the spatial runoff patterns we derived, using gridded runoff data, with those derived by L97 using spatially inhomogeneous streamflow observations, show additional patterns of coherent runoff variability in areas with sparse streamflow observations. While both our study and L97 use periods of runoff of approximately 50 years, the overlapping period is only 39 years, so the ability to definitively attribute the differences to using gridded data as opposed to observed data is limited.

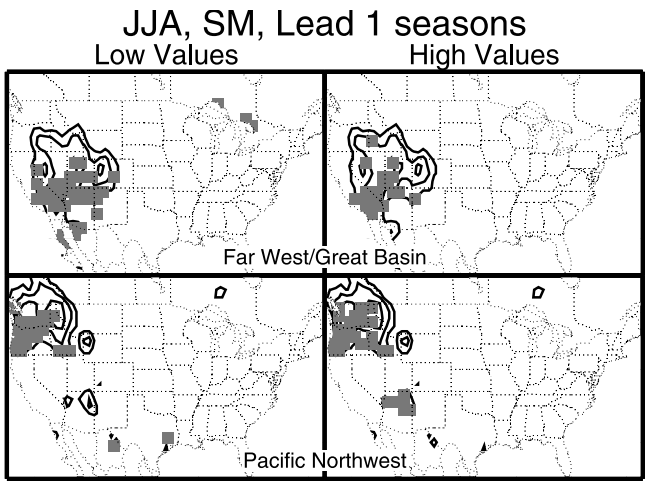

Figure 11. Same as Figure 10 but for season JJA.

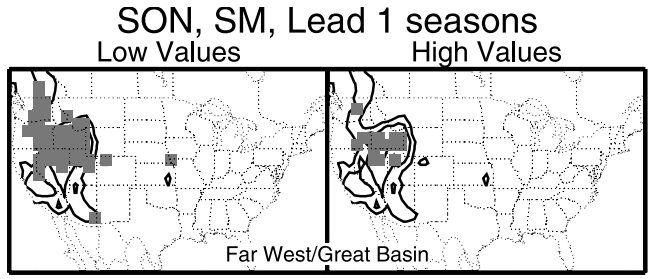

Figure 12. Same as Figure 10 but for season September–November (SON).

[44] Statistically significant relationships were identified between a variety of climate indices and to each of the patterns of runoff variability in different seasons and at different lead times. Where statistically significant relationships were identified, they are rarely associated with both phases of any climate signal, but more typically to either the positive or the negative phase. One implication of this for runoff predictability is that exploring climatic signals for potential sources of predictability requires a nonlinear analysis to avoid missing important potential runoff predictability.

[45] Characterization of the state of the land surface moisture provides an additional degree of predictability of runoff variability. Soil moisture and snow were each analyzed, using a similar technique as for the climate signals, where composites of high and low soil moisture and snow conditions were evaluated separately for their statistical relationships to the runoff patterns. Snow influences runoff as it melts, and its usefulness as a predictor is naturally related to this. It was found that for shorter lead times (an average of 1.5 month lead time) snow state provides potential predictability beyond that already available

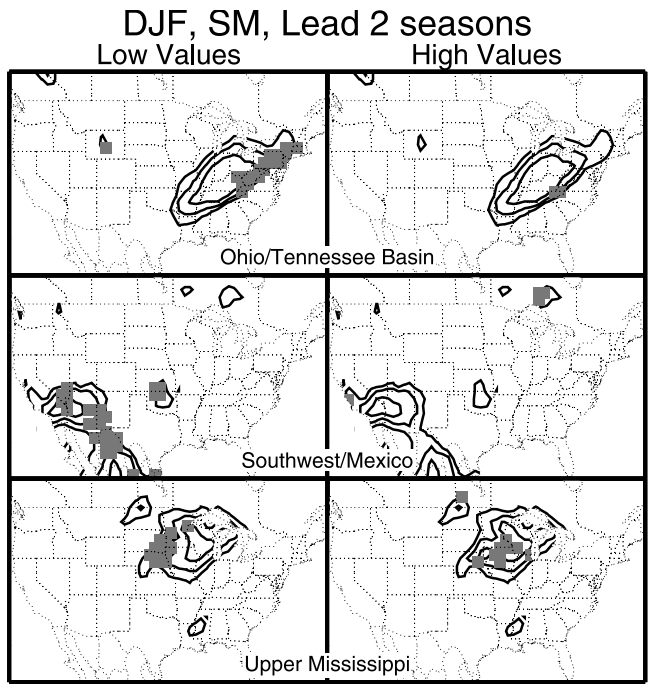

Figure 13. Same as Figure 7 but for a lead of two seasons.

through the climate signals in the Great Lakes, Far West, and Pacific Northwest regions. The summer runoff patterns in the Far West and Pacific Northwest regions are significantly related to snow state one season earlier, with low snow accumulation years providing greater runoff predictability than high. Soil moisture provides widespread predictability of winter runoff variability at short lead times. As with snow, it is more frequently a significant predictor in its dry state than wet. Though with diminished strength, soil moisture state provides predictive information for spring and summer runoff through a one season lead; for summer runoff this predictability is partially redundant, overlapping with information already available from the snow state and climate signals. At one season and longer, lead times soil moisture state has a significant impact primarily in the Midwest and Far West.

[46] On the basis of this analysis we conclude that for predicting runoff variability, knowledge of the land surface state, especially in its dry state, can provide valuable predictability as a complement to climate information for lead times of one to two seasons (i.e., up to 4.5 months lead time). For lead times greater that this, persistent climate anomalies provide the greatest opportunity for runoff prediction.

References

Baldwin, C. K. (2001), Seasonal streamflow forecasting using climate information, *Proc. West. Snow Conf.*, *69*, 95–98.

Barnston, A. G., M. Chelliah, and S. B. Goldenberg (1997), Documentation of a highly ENSO-related SST region in the equatorial Pacific, *Atmos. Ocean*, *35*, 367–383.

Barnston, A. G., M. H. Glantz, and H. Yuxiang (1999), Predictive skill of statistical and dynamical climate models in SST forecasts during 1997–98 El Niño episode and the 1998 La Niña onset, *Bull. Am. Meteorol. Soc.*, *80*, 217–243.

Bartlein, P. J. (1982), Streamflow anomaly patterns in the U.S.A. and southern Canada-1951–1970, *J. Hydrol.*, *57*, 49–63.

Bell, G. D., and M. S. Halpert (1998), Climate Assessment for 1997, *Bull. Am. Meteorol. Soc.*, *79*, S1–S50.

Cayan, D. R. (1996), Interannual climate variability and snowpack in the western United States, *J. Clim.*, *9*, 928–948.

Cayan, D. R., K. T. Redmond, and L. G. Riddle (1999), ENSO and hydrologic extremes in the western United States, *J. Clim.*, *12*, 2881–2893.

Church, J. E. (1937), The human side of snow, *Sci. Mon.*, *44*, 137–149.

Cook, E. R., D. M. Meko, D. W. Stahle, and M. K. Cleaveland (1999), Drought reconstructions for the continental United States, *J. Clim.*, *12*, 1145–1162.

DeGaetano, A. T., M. E. Hirsch, and S. J. Colucci (2002), Statistical prediction of seasonal East Coast winter storm frequency, *J. Clim.*, *15*, 1101–1117.

Derksen, C., K. Misurak, E. LeDrew, J. Piwowar, and B. Goodison (1997), Relationship between snow cover and atmospheric circulation, central North America, winter 1988, *Ann. Glaciol.*, *25*, 347–352.

Enfield, D. B., A. M. Mestas-Nunez, and P. J. Trimble (2001), The Atlantic multidecadal oscillation and it's relation to rainfall and river flows in the continental U.S., *Geophys. Res. Lett.*, *28*, 2077–2080.

Famiglietti, J. S., B. H. Braswell, and F. Giorgi (1995), Process controls and similarity in the U.S. continental-scale hydrological cycle from EOF analysis of regional climate model simulations, *Hydrol. Processes*, *9*, 437–444.

Garen, D. C. (1998), ENSO indicators and long-range climate forecasts: usage in seasonal streamflow volume forecasting in the western United States, *Eos Trans. AGU*, *79*(45), Fall Meet. Suppl., F325.

Grimmer, M. (1963), The space-filtering of monthly surface temperature anomaly data in terms of pattern, using empirical orthogonal functions, *Q. J. R. Meteorol. Soc.*, *89*, 395–408.

Guetter, A. K., and K. P. Georgakakos (1993), River outflow of the conterminous United States, 1939–1988, *Bull. Am. Meteorol. Soc.*, *74*, 1873–1891.

Hamlet, A. F., and D. P. Lettenmaier (1999), Columbia River streamflow forecasting based on ENSO and PDO climate signals, *J. Water Res. Plann. Manage.*, *125*, 333–341.

Hamlet, A. F., D. Huppert, and D. P. Lettenmaier (2002), Economic value of long-lead streamflow forecasts for Columbia River hydropower, *J. Water Res. Plann. Manage.*, *128*, 91–101.

Hare, S. R., and N. J. Mantua (2000), Empirical evidence for North Pacific regime shifts in 1977 and 1989, *Prog. Oceanogr.*, *47*, 103–145.

Higgins, R. W., A. Leetmaa, Y. Xue, and A. Barnston (2000), Dominant factors influencing the seasonal predictability of U.S. precipitation and surface air temperature, *J. Clim.*, *13*, 3994–4017.

Hornberger, G. M., et al. (2001), A plan for a new science initiative on the global water cycle, report, U.S. Global Change Res. Program, Washington, D. C.

Hurrell, J. (1995), Decadal trends in the North Atlantic Oscillation: Regional temperatures and precipitation, *Science*, *269*, 676–679.

Hurrell, J. W., Y. Kushnir, G. Ottersen, and M. Visbeck (Eds.) (2003), *The North Atlantic Oscillation: Climate Significance and Environmental Impact*, *Geophys. Monogr. Ser.*, vol. 134, 279 pp., AGU, Washington, D. C.

Kahya, E., and J. A. Dracup (1993), U.S. streamflow patterns in relation to El Niño/Southern Oscillation, *Water Resour. Res.*, *29*, 2491–2503.

Kutzbach, J. E. (1967), Empirical eigenvectors of sea-level pressure, surface temperature and precipitation complexes over North America, *J. Appl. Meteorol.*, *6*, 791–802.

Leathers, D. J., B. Yarnal, and M. A. Palecki (1991), The Pacific/North America teleconnection pattern and U.S. climate, part I: Regional temperature and precipitation associations, *J. Clim.*, *4*, 517–528.

Lettenmaier, D. P., E. F. Wood, and J. R. Wallis (1994), Hydro-climatological trends in the continental United States, 1948–1988, *J. Clim.*, *7*, 586–607.

Liang, X., D. P. Lettenmaier, E. Wood, and S. J. Burges (1994), A simple hydrologically based model of land surface water and energy fluxes for general circulation models, *J. Geophys. Res.*, *99*, 14,415–14,428.

Lin, H., and J. Derome (1998), A three-year lagged correlation between the North Atlantic Oscillation and winter conditions over the North Pacific and North America, *Geophys. Res. Lett.*, *25*, 2829–2832.

Lins, H. F. (1997), Regional streamflow regimes and hydroclimatology of the United States, *Water Resour. Res.*, *33*, 1655–1667.

Linsley, R. K., and W. C. Ackerman (1942), Method of predicting the runoff from rainfall, *Trans. Am. Soc. Civ. Eng.*, *107*, 825–846.

Mantua, N. J., S. R. Hare, Y. Zhang, J. M. Wallace, and R. C. Francis (1997), A Pacific decadal climate oscillation with impacts on salmon, *Bull. Am. Meteorol. Soc.*, *78*, 1069–1079.

Maurer, E. P., and D. P. Lettenmaier (2003), Predictability of seasonal runoff in the Mississippi River basin, *J. Geophys. Res.*, *108*(D16), 8607, doi:10.1029/2002JD002555.

Maurer, E. P., A. W. Wood, J. C. Adam, D. P. Lettenmaier, and B. Nijssen (2002), A long-term hydrologically-based data set of land surface fluxes and states for the conterminous United States, *J. Clim.*, *15*(22), 3237–3251.

McCabe, G. J., and M. D. Dettinger (1999), Decadal variations in the strength of ENSO teleconnections with precipitation in the western U.S., *Int. J. Climatol.*, *19*, 1399–1410.

National Research Council (1998), *Decade-to-Century-Scale Climate Variability and Change: A Science Strategy*, 142 pp., Natl. Acad. Press, Washington, D. C.

Overland, J. E., and R. W. Preisendorfer (1982), A significance test for principal components applied to a cyclone climatology, *Mon. Weather Rev.*, *110*, 1–4.

Parrett, C., N. B. Melcher, and R. W. James Jr. (1993), Flood discharges in the upper Mississippi River basin (1993), *U.S. Geol. Surv. Circ.*, *1120-A*, 14 pp.

Piechota, T. C., J. A. Dracup, and R. G. Fovell (1997), Western US streamflow and atmospheric circulation patterns during El Niño-Southern Oscillation, *J. Hydrol.*, *201*, 249–271.

Preisendorfer, R. W., and T. P. Barnett (1977), Significance tests for empirical orthogonal functions, paper presented at Fifth Conference on Probability and Statistics in Atmospheric Sciences, Am. Meteorol. Soc., Las Vegas, Nev.

Rasmussen, E. M., and J. M. Wallace (1983), Meteorological aspects of the El Niño/Southern Oscillation, *Science*, *222*, 1195–1202.

Rice, R. M. (1967), Multivariate methods useful in hydrology, paper presented at International Hydrology Symposium, Colo. State Univ., Ft. Collins, Sept.

Richman, M. B. (1986), Rotation of principal components, *J. Clim.*, *6*, 293–335.

Rogers, A. N., D. H. Bromwich, E. N. Sinclair, and R. I. Cullather (2001), The atmospheric hydrologic cycle over the Arctic basin from reanalyses, part 2, Interannual variability, *J. Clim.*, *14*, 2414–2429.

Rohli, R. V., A. J. Vega, M. R. Binkley, S. D. Britton, H. E. Heckman, J. M. Jenkins, Y. Ono, and D. E. Sheeler (1999), Surface and 700 hPa atmospheric circulation patterns for the Great Lakes basin and eastern North America and relationship to atmospheric telecommunications, *J. Great Lakes Res.*, *25*, 45–60.

Snyder, W. M. (1962), Some possibilities for multivariate analysis in hydrologic studies, *J. Geophys Res.*, *67*, 721–729.

Thompson, D. W. J., and J. M. Wallace (1998), The Arctic Oscillation signature in the wintertime geopotential height and temperature fields, *Geophys. Res. Lett.*, *25*, 1297–1300.

Thompson, D. W. J., and J. M. Wallace (2000), Annular modes in the extratropical circulation. Part I: Month-to-month variability, *J. Clim.*, *13*, 1000–1016.

Trenberth, K. E. (1997), The definition of El Niño, *Bull. Am. Meteorol. Soc.*, *78*, 2771–2777.

Trenberth, K. E., and J. Hurrell (1994), Decadal atmosphere-ocean variations in the Pacific, *Clim. Dyn.*, *9*, 303–319.

Wallis, J. R. (1965), Multivariate statistical methods in hydrology—A comparison using data of known functional relationship, *Water Resour. Res.*, *1*, 447–461.

Wettstein, J. J., and L. O. Mearns (2002), The influence of the North Atlantic-Arctic Oscillation on mean, variance, and extremes of temperature in the northeastern United States and Canada, *J. Clim.*, *15*, 3586–3600.

Wittrock, V., and E. A. Ripley (1999), The predictability of autumn soil moisture levels on the Canadian prairies, *Int. J. Climatol.*, *19*, 271–289.

Wong, S. T. (1963), A multivariate statistical model for predicting mean annual flood in New England, *Ann. Assoc. Am. Geogr.*, *53*, 298–311.

Wood, A. W., E. P. Maurer, A. Kumar, and D. P. Lettenmaier (2002), Long range experimental hydrologic forecasting for the eastern U.S., *J. Geophys. Res.*, *107*(D20), 4429, doi:10.1029/2001JD000659.

D. P. Lettenmaier, Department of Civil and Environmental Engineering, University of Washington, Box 352700, Seattle, WA 98195-2700, USA.

N. J. Mantua, Climate Impacts Group, Joint Institute for the Study of the Atmosphere and Ocean, University of Washington, Box 354235, Seattle, WA 98195-4235, USA.

E. P. Maurer, Civil Engineering Department, Santa Clara University, 500 El Camino Real, Santa Clara, CA 95053-0563, USA. (emaurer@engr.scu.edu)